Angular-Stability Low-Profile Miniaturized Frequency Selective Surface Based on Complementary Structure

Wenxing Li and Yuanyuan Li[*]

Abstract—A new architecture for a low-profile miniaturized-element frequency selective surface based on complementary structure capable of providing a high angular stable performance is proposed. The proposed FSS is composed of an array of convoluted cross dipoles and its complementary slots pattern that is separated by a thin dielectric substrate. An equivalent circuit model for this FSS is presented to provide a deep insight into the mechanism of reducing the unit size by shifting and lengthening the dipoles. With the use of this method, the FSS unit cell size has been significantly reduced to only $0.0085\lambda \times 0.0085\lambda$, and the thickness is 0.000093λ, where λ represents the resonant wavelength in free space. Moreover, the proposed FSS achieves good stability in the scope of incidence angles of 86 degrees for both TE and TM polarizations. Besides, the length of the dipoles can tune the resonant frequency.

1. INTRODUCTION

Frequency selective surface (FSS) has been intensively investigated for their wide range of application in military and commercially areas over the past few decades. FSS is a two-dimensional periodic structure composed of periodically arranged metallic patches or aperture elements which are etched on the surface of the dielectric substrate. It can act as a spatial filter which has a selective effect on the incident angle, polarization and frequency of electromagnetic wave [1, 2]. Frequency selective surface has been widely used as radar radome [3], antenna reflector [4, 5], polarization converter [6], microwave absorber [7], etc. In practical applications, it is difficult to arrange sufficient number of elements in the limited region and make them act as an infinite FSS [8, 9]. Therefore, miniaturized FSS is proposed and investigated extensively. Methods of several types have been implemented to design miniaturized FSS in the past, of which using convoluted and interwoven technique [10–12], loading via technique [13, 14], capacitive surface and inductive surface coupling technique [15, 16], and loading lumped elements technique [17] are the prominent. The principle of them is to increase the equivalent inductance and capacitance of the FSS. It is a flexible and obvious method to reduce the unit size by loading lumped elements. Liu et al. proposed an FSS loaded with inductance and capacitance and has a dimension of $0.028\lambda \times 0.028\lambda$, where λ is the wavelength in free space at resonant frequency [17]. However, this method requires bulk lumped elements, which increases the difficulty of fabrication. In recent years, designing a miniaturized FSS without loading has attracted more and more attentions. In [10], a miniaturized FSS realized by symmetrically bending the edges of square loop aperture element has been proposed. The unit size is $0.0538\lambda \times 0.0538\lambda$. In [13], a 2.5-dimension miniaturized FSS consisting of a planar meandering line and a vertical via-based meandering line has been proposed with a $0.033\lambda \times 0.033\lambda$ dimension. In [12], an interwoven and convoluted dipoles were used to achieve a miniaturized FSS, and the element size is $0.0094\lambda \times 0.0094\lambda$. In [16], Lin et al. proposed a miniaturized FSS based on the coupling method, and the unit cell dimension is $0.0094\lambda \times 0.0094\lambda$. One common feature of the aforementioned

* Corresponding author: Yuanyuan Li (lyy008@hotmail.com).
The authors are with the College of Information and Communications Engineering, Harbin Engineering University, Harbin 150001, China.

FSSs is that although they achieve the miniaturization, the angular stability is somewhat low despite their achievement of miniaturization. Therefore, the design of a highly angular stability, low profile miniaturized FSS is still challenging.

In this paper, an angular stable low profile miniaturized FSS with the unit cell dimension of $0.0085\lambda \times 0.0085\lambda$ is proposed using convoluted and coupling technologies. Compared to previous works, the FSS achieves better performance of angular stability when the incident angle is up to 86 degrees for both TE and TM polarizations. It is also miniaturized and has low profile. The design process and results of the proposed FSS are presented and discussed in following sections.

2. DESIGN OF COMPLEMENTARY MINIATURIZED FSS

2.1. Topology of FSS and Working Principle

Figure 1(a) shows a 3-D view of the complementary miniaturized FSS, consisting of two metal layers separated by a dielectric substrate with a thickness of h. The main challenge in design of the miniaturized FSS is decreasing the unit cell in dimension for reducing the sensitivity of the polarization and the incident angle. With the view to overcoming it, the unit cell is designed symmetrically in x and y directions. Hence, the period of the topology in x and y directions is equal $(D_x = D_y = D)$, and the unit cell on the top layer uses a convoluted cross dipole structure, while the unit cell on the bottom layer is the complementary slot of the unit cell on the top layer.
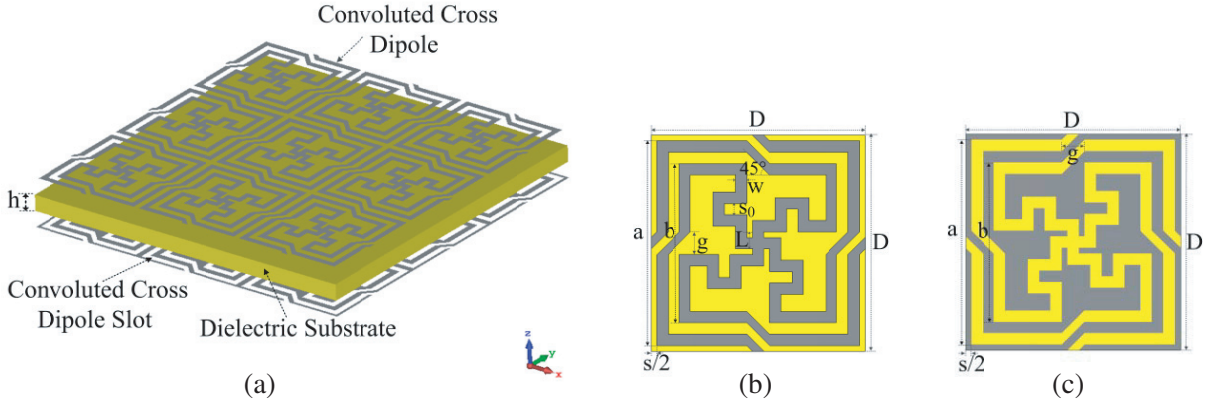

Figure 1. Topology of the proposed miniaturized FSS. (a) 3-D view of the FSS. (b) Unit cell on top layer. (c) Unit cell on bottom layer $D = 5.7\,\text{mm}$, $a = 5.4\,\text{mm}$, $b = 4.2\,\text{mm}$, $w = 0.3\,\text{mm}$, $s = 0.3\,\text{mm}$, $s0 = 0.3\,\text{mm}$, $L = 0.6\,\text{mm}$, $g = 0.6\,\text{mm}$, $h = 0.508\,\text{mm}$.

Figure 2 shows the equivalent circuit model to the miniaturized FSS which provides further insight into the FSS behavior. The equivalent circuit model of this FSS is illustrated in Fig. 2(a), which is valid for incident EM wave of vertical polarization along x direction. In the circuit model, the top layer is modelled with a hybrid resonator composed of L_1, C_1 and L_s as shown in the left part of Fig. 2(a). The parallel resonator composed of L_1 and C_1 equivalents to the convoluted cross dipole resonator. And the inductance between the two adjacent unit cells is represented by series inductor L_s. L_1 is the equivalent inductance of convoluted cross dipole, arm and C_1 denotes the capacitance between the dipole arms in one unit cell. As the complementary slot of unit cell on the bottom layer, the equivalent circuit consists of a series LC resonator (L_2 and C_2) connected in parallel with a capacitor C_s as shown on the right in Fig. 2(a). C_2 is the capacitance of convoluted cross dipole slot and C_s the capacitance between adjacent cells. L_2 denotes the inductance of the metal on bottom layer. Fig. 2(b) is the simplified equivalent circuit model disregarding the effect of L_s and C_s on the frequency response. In conclusion, therefore, the FSS has produced a passband over the low frequencies and a stopband at high frequencies. The
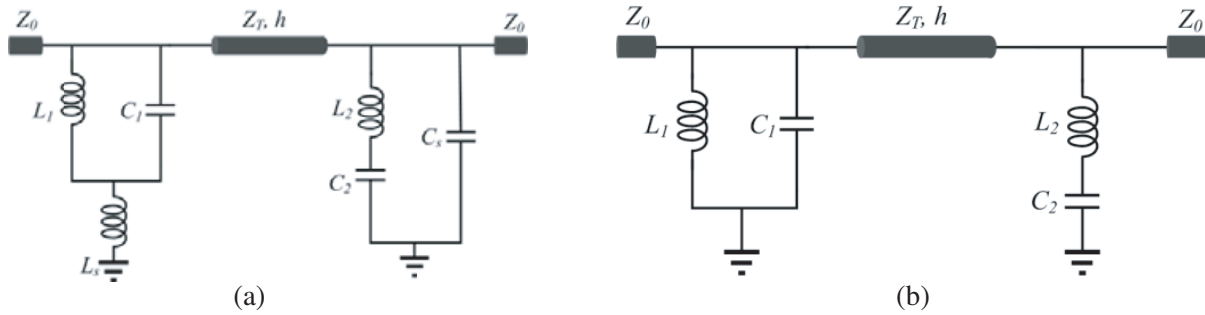
Figure 2. (a) Equivalent circuit model of the proposed FSS. (b) Simplified equivalent circuit model of (a).

resonant frequencies are calculated as

$$f_0 = \frac{1}{2\pi\sqrt{L_1(C_1 + C_2)}} \tag{1}$$

$$f_z = \frac{1}{2\pi\sqrt{L_2 C_2}} \tag{2}$$

The dielectric substrate, sandwiched between two metal layers, is equivalent to a short transmission line whose length is h. Its impedance is $Z_T = Z_0/\sqrt{\varepsilon_r}$, where Z_0 is the wave impedance in free space and ε_r the relative permittivity of the dielectric substrate.

2.2. Simulation and Experimental Verification

The miniaturized FSS has been fabricated and measured. The prototype has two metal layers fabricated on two sides of a 0.508 mm thick RO4350B substrate whose permittivity is 3.48. It contains 50×50 cells in a 285 mm $\times$ 285 mm region. Fig. 3 shows photographs of FSS and the measurement setup. The measurement results started from 1 GHz is because the horn antennas for testing operate at 1–8 GHz.

Figure 4 compares the measurement and simulated results calculated by CST-MWS and equivalent circuit model. As illustrated, the FSS transmits the signal at 1.75 GHz, while reflecting the unnecessary signal at 3.51 GHz, and the simulation results are in good agreement with the measurement ones. The fractional bandwidth is 45%. The unit size is $0.041\lambda \times 0.041\lambda$, and the thickness is 0.0037λ, where λ is the resonate wavelength in free space. We reach the conclusion that this FSS demonstrates a good performance of miniaturization and low profile. The frequency response of the FSS at different incident angles has also been examined.
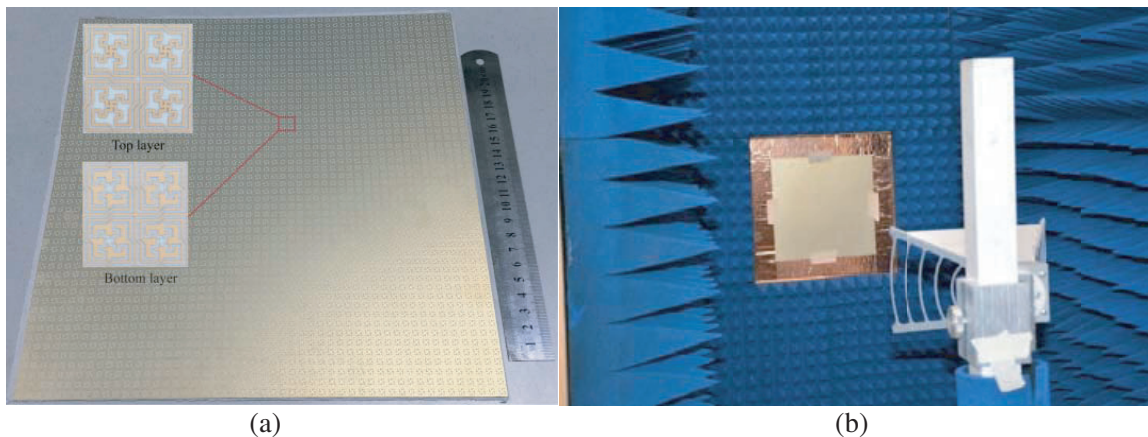

Figure 3. (a) Photograph of the fabricated FSS prototype. (b) Photograph of measurement setup.
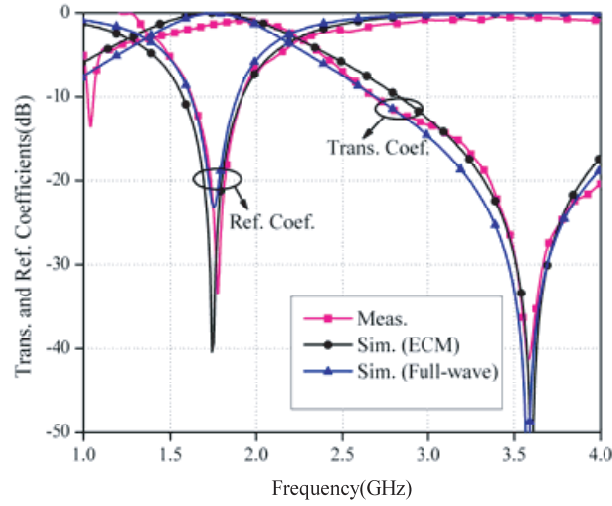
Figure 4. Simulated and measurement results of miniaturized FSS.

Figure 5 shows the measurement results as well as the simulated ones in comparison. The frequency response is extremely stable under different angles for both TE and TM polarizations when the incident angle is changed from 0° to 60°. The resonant frequency shows fair stability even when the incident angle was larger than 80 degrees for TE polarization. For TM polarization, however, the deviations of resonant frequency are 5.13% and 26.5% when the incident angles are 80 and 86 degrees, respectively. It is observed that the bandwidth decreases with the increase of incident angle for TE polarization, whereas the TM polarization is the opposite. This observed changes can be illustrated by the variation of wave impedance [18]. In the case of TE polarization, the wave impedance ($Z_{TE} = Z_0/\cos\theta$) increases with the increase of the incident angle, and then the quality factor of the filter's resonator decreases, which causes the reduction of the bandwidth of resonator. For TM polarization, the wave impedance ($Z_{TM} = Z_0 \cos\theta$) decreases with the increase of the incident angle, which causes the decline of the quality factor of filter's resonator, and the bandwidth of the FSS is broadened.

3. MODIFIED MINIATURIZED FSS

It is known that reducing the unit size is to increase the value of the equivalent inductance or capacitance of the FSS element. In this section, investigations on reducing the unit size and improving the angular stability are carried out. First, the unit size is notably decreased by increasing the capacitance of the FSS. Then the equivalent inductance is increased by lengthening the convoluted cross dipoles.

3.1. Miniaturized FSS Based on Shifting Method

The methods of increasing the equivalent capacitance include reducing the distance between slots in each layer, increasing the dielectric constant and reducing the substrate thickness. Besides the aforementioned methods, the capacitance also lies on the overlapping area between the two metal layers. In our design, we use the shifting method to make an offset between the top and bottom metal layers to increase the equivalent capacitance. The top layer is shifted by $D/2$ along x and y simultaneously as shown in Fig. 6.

Figure 7 shows the modified structure and its equivalent circuit to the capacitive structure. We observe that the four overlapping parts between the top and bottom metal layers form parallel plate capacitors of C_0. It may be approximated by the following equation [15]:

$$C_0 = \frac{\varepsilon_0 \varepsilon_{eff} A}{h} \qquad (3)$$

where, A is the overlapping area between the two metal layers, h the thickness of the dielectric substrate between the two metal layers, and $\varepsilon_{eff} = (1+\varepsilon_r)/2$ the effective dielectric constant [19]. As observed,
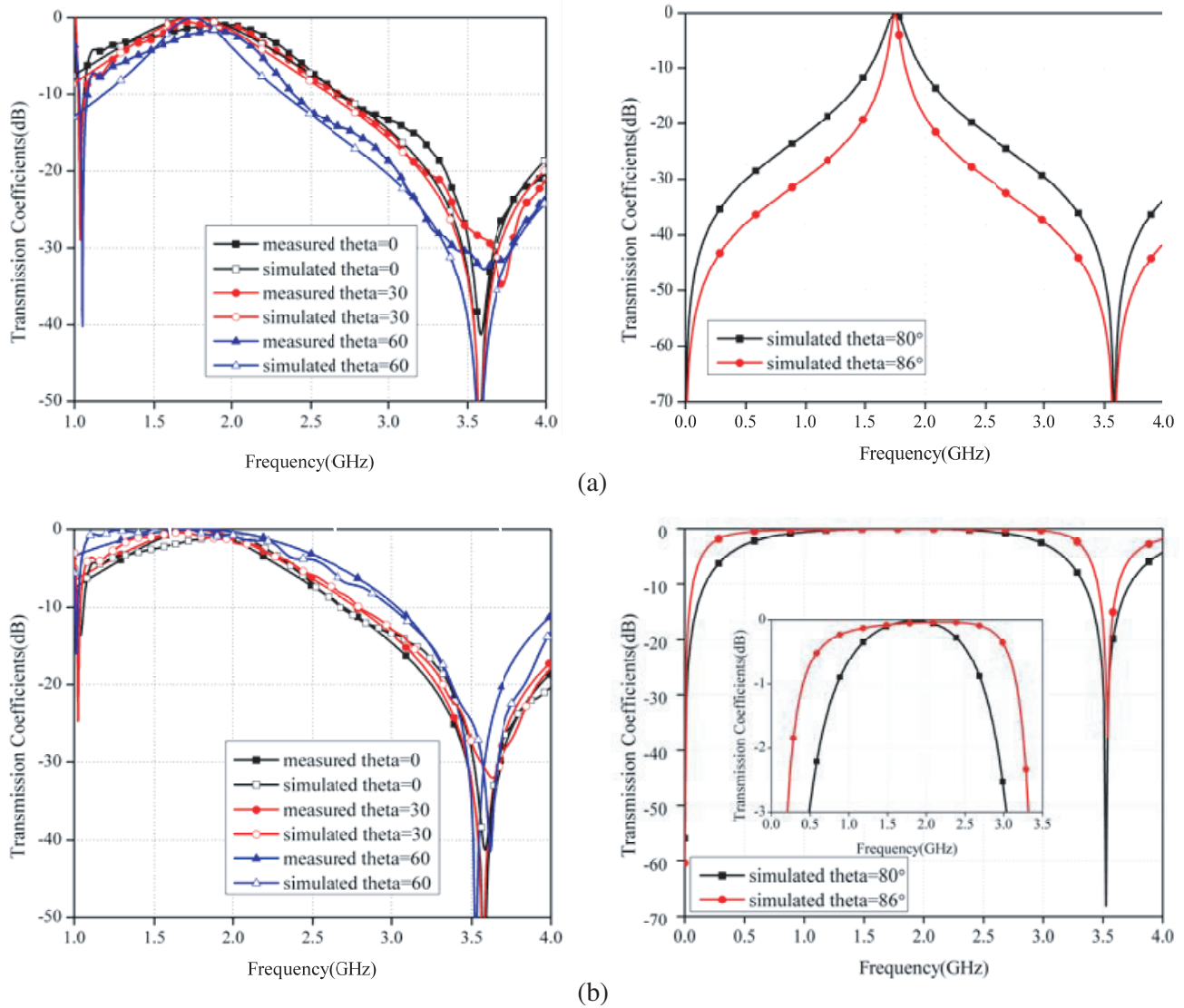
Figure 5. Measured and simulated transmission coefficients of FSS for oblique incident angles. (a) TE polarization. (b) TM polarization.
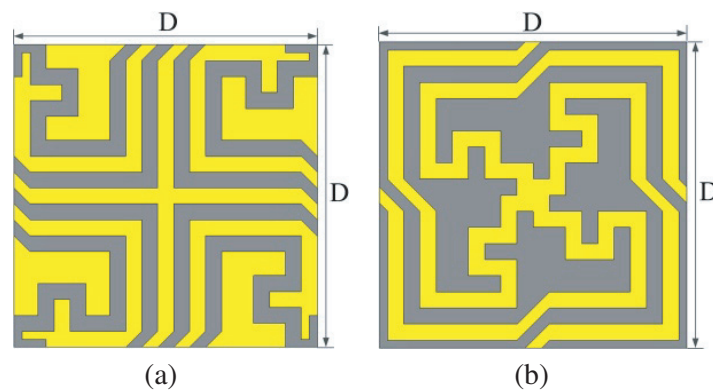

Figure 6. Topology of modified miniaturized FSS based on shifting method. $D = 5.7\,\text{mm}$. (a) Top layer. (b) Bottom layer.
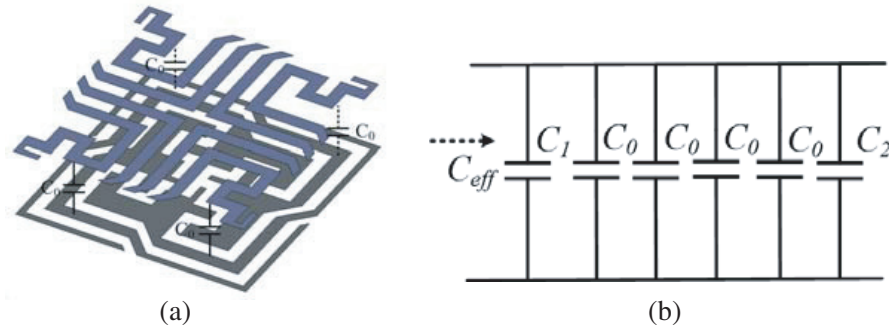
Figure 7. (a) The capacitive structure. (b) The equivalent circuit model of the capacitive structure.

the equivalent capacitance can be calculated by the following formula:

$$C_{eff} = C_1 + 4C_0 + C_2 \tag{4}$$

Therefore, the unit size is decreased by increasing the equivalent capacitance which is proportional to the overlapping area and is inversely proportional to the thickness of the dielectric substrate. The frequency response is calculated by the CST-MWS. The relative dielectric constant is 4.4, and the thickness is 0.101 mm. The resonant frequency of the modified FSS is reduced to 0.66 GHz, and the unit size is significantly miniaturized to $0.013\lambda \times 0.013\lambda$.

3.2. Miniaturized FSS Based on Lengthening the Dipoles

To further reduce the unit size of the FSS, the convoluted cross dipoles presented in Fig. 6 are lengthened to increase the equivalent inductance of the FSS as shown in Fig. 8. P is the dimension of the modified FSS.
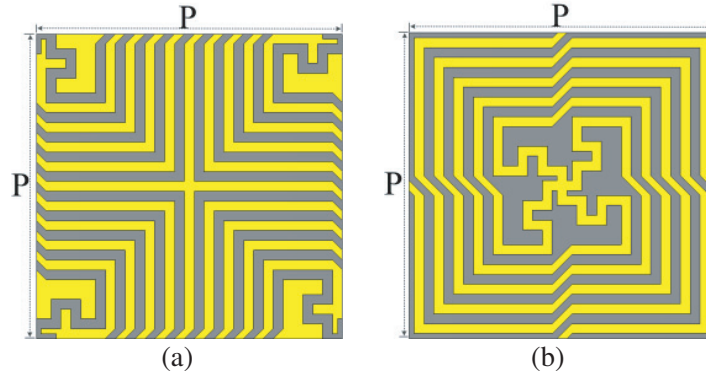

Figure 8. Topology of modified FSS based lengthening the convoluted cross dipoles. $P = 9.3$ mm. (a) Top layer. (b) Bottom layer.

The modified FSS was simulated in CST microwave studio, and its frequency response was calculated. The dielectric constant of the dielectric substrate is 4.4, and the thickness of h is 0.101 mm. Fig. 9 shows the comparison between transmission coefficient of the modified FSS and the FSS presented in Section 2. As observed, the center frequency of the modified FSS is reduced to 0.276 GHz. Compared to the result in Fig. 4, the element size is drastically reduced to $0.0085\lambda \times 0.0085\lambda$, and the thickness is $0.000093\lambda \times 0.000093\lambda$, where λ is the wavelength in free space. Obviously, the modified FSS exhibits good performance of miniaturization and low profile. However, the reduction of the unit size is at the expense of the cost of bandwidth as shown in Fig. 9. The fractional bandwidth is reduced from 45% to 16.4%. The frequency response of the modified FSS under different incident angles is also calculated
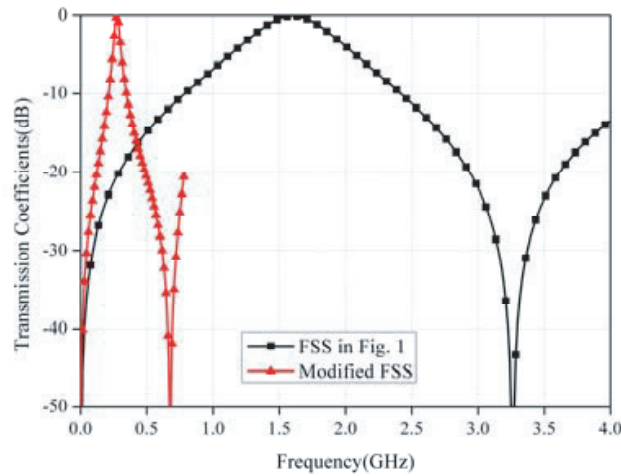
Figure 9. Comparison of transmission coefficients of the modified FSS and the FSS presented in Fig. 1.

as presented in Fig. 10. In addition, the transmission properties of angular stability and polarization independence are summarized in Table 1. As observed, the response is stable when the incident angles change from 0° to 86° for both TE and TM polarizations with a deviation of merely 0.7% for TM polarization when the incident angle is 86°. Comparisons of the element size and maximum incident angle between the modified FSS and the previous works are presented in Table 2. From Table 2, it

Table 1. Data for TE and TM incident angles.

Incident angle	TE Polarization		TM Polarization	
	f_{01}(GHz)	f_{01}deviation(%)	f_{01}(GHz)	f_{01}deviation(%)
0°	0.276	0	0.276	0
30°	0.276	0	0.276	0
60°	0.276	0	0.276	0
80°	0.276	0	0.276	0
86°	0.276	0	0.276	0.7

Table 2. Results comparison to other miniaturized FSS structures.

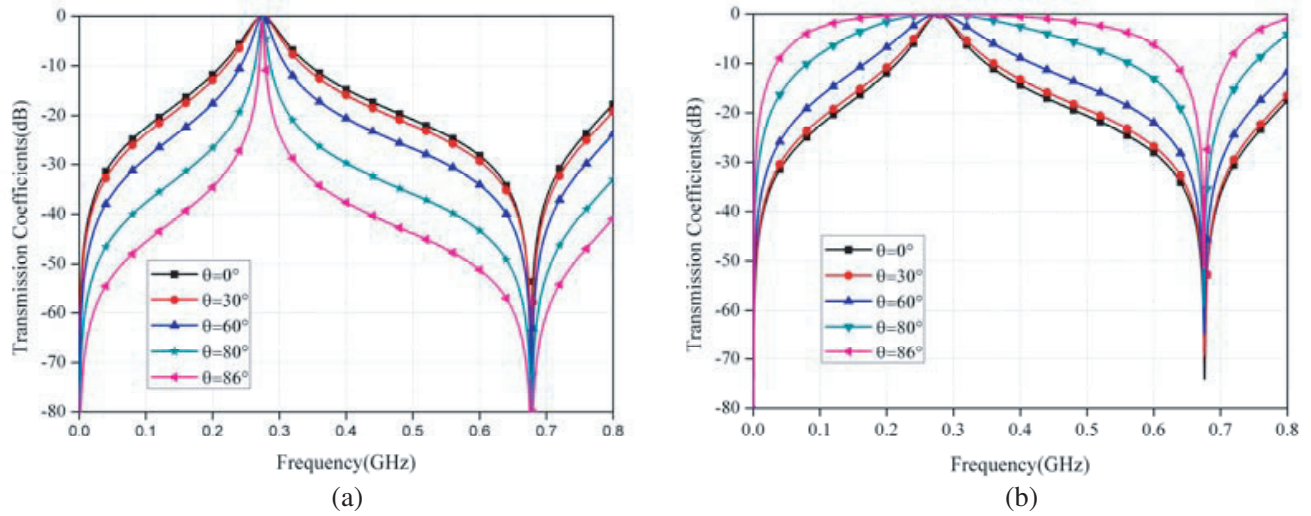| ε_r	element	Unit size (λ)	Thickness (λ)	Incident angle	Center frequency (GHz)
2.2	Ref. [14]	0.067	0.0013	80°	3.33
	This FSS	0.012	0.0004	86°	0.38
3	Ref. [12]	0.018	0.0048	60°	2.9
	This FSS	0.01	0.00011	86°	0.33
4.4	Ref. [13]	0.0094	0.000047	75°	0.14
	This FSS	0.0085	0.000093	86°	0.276
5	Ref. [11]	0.0538	0.0088	60°	1.647
	This FSS	0.008	0.00027	86°	0.68
10.2	Ref. [15]	0.0094	0.00056	60°	0.188
	This FSS	0.0059	0.00021	80°	0.19

Figure 10. Transmission coefficients of the modified FSS under different incident angles. (a) TE polarization. (b) TM polarization.

is seen that the design exhibits more miniaturized performance and produces a better angular stable response.

3.3. Sensitivity of the Response to Dielectric Constant and Substrate Thickness

According to the working principle of the modified FSS, the parameters of the dielectric substrate directly affect the frequency response of the FSS. Fig. 11 shows the results of the modified FSS with respect to the thickness of the dielectric substrate. The resonant frequency increases with the thickness. This is because the thickness is equivalent to the space of a parallel plate capacitor. It is inversely proportional to equivalent capacitance.
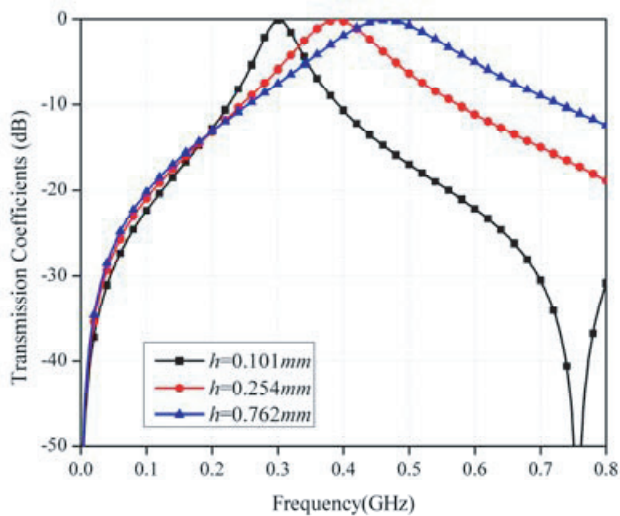

Figure 11. Transmission coefficients of the modified FSS for different thickness.
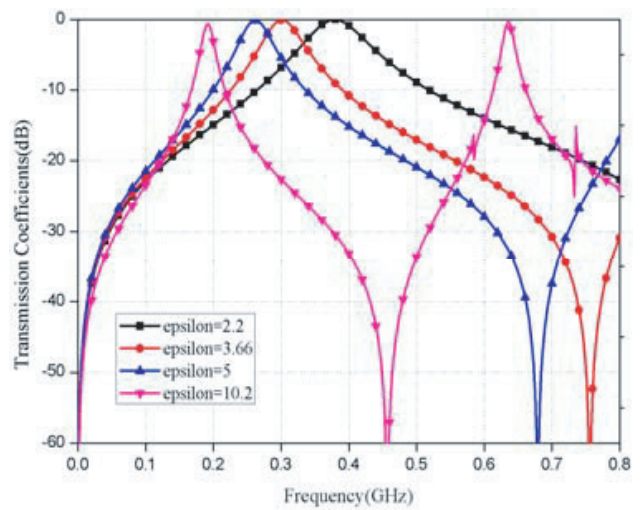

Figure 12. Transmission coefficients of the modified FSS for different dielectric constant.

4. CONCLUSIONS

In this paper, a novel, low-profile and miniaturized frequency selective surface with a high angular stability based on complementary structure is proposed. A method of shifting top layer and lengthening the dipoles to reduce the element size is presented and validated. The FSS has a much better miniaturization and low profile performance than other elements proposed in previous literatures with the unit size of $0.0085\lambda \times 0.0085\lambda$ and thickness of 0.000093λ. The FSS exhibits excellent angular stability for both TE and TM polarizations up to $86°$. In addition, the element size is able to be further reduced by applying this method.

ACKNOWLEDGMENT

REFERENCES

1. Ben, A., *Frequency Selective Surface — Theory and Design*, Vol. 319, 315, A Wiley-Interscience Publication, 2000.
2. Farahat, A. E., K. F. A. Hussein, and N. M. El-Minyawi, "Spatial filters for linearly polarized antennas using free standing frequency selective surface," *Progress In Electromagnetics Research M*, Vol. 2, 167–188, 2008.
3. Chen, Q. and Y. Fu, "A planar stealthy antenna radome using absorptive frequency selective surface," *Microwave and Optical Technology Letters*, Vol. 56, 1788–1792, 2014.
4. Edalati, A. and K. Sarabandi, "Reflectarray antenna based on grounded loop-wire miniaturised-element frequency selective surfaces," *IET Microwaves, Antennas & Propagation*, Vol. 8, 973–979, 2014.
5. Chatterjee, A. and S. Parui, "Performance enhancement of a dual-band monopole antenna by using a frequency selective surface-based corner reflector," *IEEE Transactions on Antennas and Propagation*, 1, 2016.
6. Gangwar, D., S. Das, R. L. Yadava, and B. K. Kanaujia, "Circularly polarized inverted stacked high gain antenna with frequency selective surface," *Microwave and Optical Technology Letters*, Vol. 58, 732–740, 2016.
7. Wang, H., P. Kong, W. Cheng, W. Bao, X. Yu, L. Miao, et al., "Broadband tunability of polarization-insensitive absorber based on frequency selective surface," *Sci. Rep.*, Vol. 6, 23081, 2016.
8. Oraizi, H. and M. Afsahi, "Design of metamaterial multilayer structures as frequency selective surfaces," *Progress In Electromagnetics Research C*, Vol. 6, 115–126, 2009.
9. Guo, C., H.-J. Sun, and X. Lv, "A novel dualband frequency selective surface with periodic cell perturbation," *Progress In Electromagnetics Research B*, Vol. 9, 137–149, 2008.
10. Li, W., C. Wang, Y. Zhang, and Y. Li, "A miniaturized frequency selective surface based on square loop aperture element," *International Journal of Antennas and Propagation*, Vol. 2014, 1–6, 2014.
11. Zhao, P.-C., Z.-Y. Zong, W. Wu, and D.-G. Fang, "A convoluted structure for miniaturized frequency selective surface and its equivalent circuit for optimization design," *IEEE Transactions on Antennas and Propagation*, Vol. 64, 2963–2970, 2016.
12. Yan, M., S. Qu, J. Wang, H. Ma, J. Zhang, W. Wang, et al., "A single layer ultra-miniaturized FSS operating in VHF," *Photonics and Nanostructures — Fundamentals and Applications*, Vol. 17, 1–9, Nov. 2015.

13. Yu, Y.-M., C.-N. Chiu, Y.-P. Chiou, and T.-L. Wu, "A novel 2.5-dimensional ultraminiaturized-element frequency selective surface," *IEEE Transactions on Antennas and Propagation*, Vol. 62, 3657–3663, 2014.

14. Hussain, T., Q. Cao, J. Kayani, and I. Majid, "Miniaturization of frequency selective surfaces using 2.5-dimensional knitted structures: Design and synthesis," *IEEE Transactions on Antennas and Propagation*, 1, 2017.

15. Azemi, S. N., K. Ghorbani, and W. S. T. Rowe, "Angularly stable frequency selective surface with miniaturized unit cell," *IEEE Microwave and Wireless Components Letters*, Vol. 25, 454–456, Jul. 2015.

16. Lin, B.-Q., S.-H. Zhao, X.-Y. Da, Y.-W. Fang, J.-J. Ma, and Z.-H. Zhu, "Design of a miniaturized-element frequency selective surface," *Microwave and Optical Technology Letters*, Vol. 57, 2572–2576, 2015.

17. H. L. Liu, K. L. Ford, and R. J. Langley, "Design methodology for a miniaturized frequency selective surface using lumped reactive components," *IEEE Transactions on Antennas and Propagation*, Vol. 57, 2732–2738, 2009.

18. Al-Joumayly, M. A. and N. Behdad, "Low-profile, highly-selective, dual-band frequency selective surfaces with closely spaced bands of operation," *IEEE Transactions on Antennas and Propagation*, Vol. 58, 4042–4050, 2010.

19. Momeni Hasan Abadi, S. M. A., L. Meng, and N. Behdad, "Harmonic-suppressed miniaturized-element frequency selective surfaces with higher order bandpass responses," *IEEE Transactions on Antennas and Propagation*, Vol. 62, 2562–2571, 2014.